HSP90 inhibitor geldanamycin reverts IL-13– and IL-17–induced airway goblet cell metaplasia

Alejandro A. Pezzulo,[1,2] Rosarie A. Tudas,[1,2] Carley G. Stewart,[1,2] Luis G. Vargas Buonfiglio,[1] Brian D. Lindsay,[1] Peter J. Taft,[1,2] Nicholas D. Gansemer,[1,2] and Joseph Zabner[1,2]

[1]Department of Internal Medicine, Roy J. and Lucille A. Carver College of Medicine, and [2]Pappajohn Biomedical Institute, University of Iowa, Iowa City, Iowa, USA.

Goblet cell metaplasia, a disabling hallmark of chronic lung disease, lacks curative treatments at present. To identify novel therapeutic targets for goblet cell metaplasia, we studied the transcriptional response profile of IL-13–exposed primary human airway epithelia in vitro and asthmatic airway epithelia in vivo. A perturbation-response profile connectivity approach identified geldanamycin, an inhibitor of heat shock protein 90 (HSP90) as a candidate therapeutic target. Our experiments confirmed that geldanamycin and other HSP90 inhibitors prevented IL-13–induced goblet cell metaplasia in vitro and in vivo. Geldanamycin also reverted established goblet cell metaplasia. Geldanamycin did not induce goblet cell death, nor did it solely block mucin synthesis or IL-13 receptor–proximal signaling. Geldanamycin affected the transcriptome of airway cells when exposed to IL-13, but not when exposed to vehicle. We hypothesized that the mechanism of action probably involves TGF-β, ERBB, or EHF, which would predict that geldanamycin would also revert IL-17–induced goblet cell metaplasia, a prediction confirmed by our experiments. Our findings suggest that persistent airway goblet cell metaplasia requires HSP90 activity and that HSP90 inhibitors will revert goblet cell metaplasia, despite active upstream inflammatory signaling. Moreover, HSP90 inhibitors may be a therapeutic option for airway diseases with goblet cell metaplasia of unknown mechanism.

Introduction

Human lungs constantly interact with the environment. In some individuals, various environmental exposures cause chronic mucus hypersecretion, leading to disability and reduced quality of life (1–3). Goblet cell metaplasia is the accumulation of mucin-secreting goblet cells in the airway (reviewed in ref. 4) and is a hallmark of lung diseases with mucus hypersecretion (5).

Lung disease with goblet cell metaplasia can be caused by various triggers: smoke from cigarettes or biomass fuels can trigger chronic bronchitis; environmental allergens can trigger asthma; and mutations of cystic fibrosis transmembrane conductance regulator (*CFTR*) can trigger infection and inflammation in cystic fibrosis. These triggers affect epithelial, immune, and other cells types in the airways. Multiple cellular pathways modulate goblet cell metaplasia, including the IL-4/IL-13 pathway (6–11), the NOTCH pathway (4, 12–18), the IL-17 neutrophilic inflammation pathway (19–24), and the EGFR/ERBB protein family pathway (25). In addition, inflammatory pathways may complement or counteract each other (26–28).

Various pathways may drive distinct asthma endotypes (29–32). In 50% of individuals with asthma, IL-4/IL-13 signaling drives the Th2-high asthma endotype (33–36), which is the best-characterized chronic lung disease associated with goblet cell metaplasia. In contrast, in individuals with Th2-low asthma, chronic bronchitis, or cystic fibrosis, the mechanisms of goblet cell metaplasia are poorly understood. Targeted asthma therapy trials involving antibodies against IgE, IL-4/IL-13, IL-4R, IL-5, IL-5R, IL-17, and others (37) have had variable outcomes (38), probably because they target inflammatory pathways that interact with each other in complex ways.

The treatment of chronic mucus hypersecretion is challenging. Mucus hypersecretion may last a few weeks in upper respiratory infections (39, 40) or over a decade in chronic bronchitis, even after smoking cessation (41). Inflammatory cytokines may contribute to chronic mucus hypersecretion by inducing epigenetic changes that perpetuate goblet cell metaplasia (42, 43). Mucolytics and expectorants target the viscoelastic properties of mucus and improve symptoms, but they do not treat goblet cell metaplasia. On the other hand, inhaled corticosteroids improve asthma and can prevent goblet cell metaplasia (44). However, corticosteroids have limited efficacy in Th2-low asthma and chronic bronchitis. Other therapies, such as those involving MAPK inhibitors, are being studied (45, 46). There are currently no curative treatments for chronic goblet cell metaplasia and mucus hypersecretion.

We used a perturbation-response profile connectivity approach to identify novel treatments for goblet cell metaplasia. Perturbation-response connectivity databases track how the transcriptional response of cell lines changes in response to drug exposure and can identify drugs that mimic or revert a transcriptional response of interest (47–51). The perturbation-response connectivity approach can be useful despite incomplete knowledge about the mechanism driving the disease and has identified the heat shock protein 90 (HSP90) inhibitor geldanamycin as a candidate for reverting airway goblet cell metaplasia. Our tests determined that geldanamycin prevented IL-13–induced goblet cell metaplasia in human airway epithelia in vitro and in murine airway epithelia in vivo. Moreover, geldanamycin reverted established

Conflict of interest: The authors have declared that no conflict of interest exists.

Submitted: July 12, 2018; **Accepted:** November 20, 2018.
Reference information: *J Clin Invest*. 2019;129(2):744–758.
https://doi.org/10.1172/JCI123524.

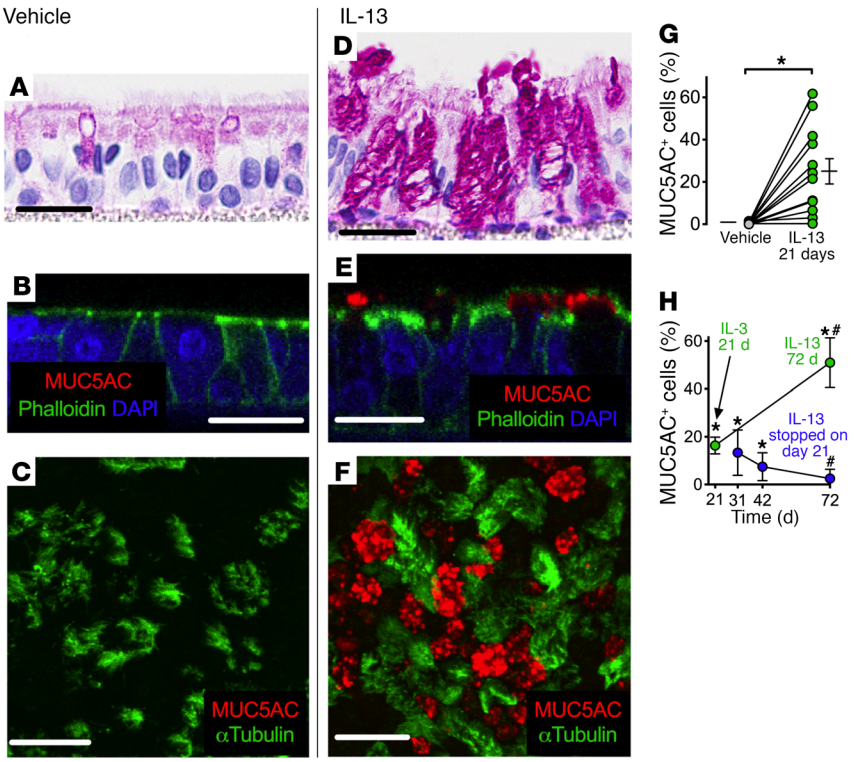

Figure 1. IL-13 induces goblet cell metaplasia in primary cultures of human airway epithelia. Primary human airway epithelia grown at the air-liquid interface were exposed to vehicle (**A**–**C**) or 20 ng/ml human recombinant IL-13 (**D**–**F**) for 21 days. dPAS staining (**A** and **D**) was performed to quantify goblet cells and other cell types. Immunofluorescence (**B** and **E** show orthogonal reconstruction, **C** and **F** show en face stack) was performed to quantify goblet (MUC5AC-positive) and ciliated (acetylated α-tubulin–positive) cells. Intracellular localization of MUC5AC was confirmed with phalloidin staining. (**G**) Percentage of MUC5AC-positive cells after 21 days of exposure to IL-13; each point corresponds to epithelia from a different donor (n = 12 biological replicates). (**H**) To determine the persistence of goblet cells, IL-13 exposure was terminated after 21 days, and goblet cells were quantified 10, 21, and 50 days after IL-13 treatment (experimental days 31, 42, and 71, respectively). Scale bars: 20 μm. n = 6 biological replicates. Pooled data are shown as the mean ± SEM. *P < 0.01 versus the corresponding vehicle-treated group; #P < 0.05 versus 21-day IL-13 treatment group; 2-tailed, paired t test.

IL-13–induced goblet cell metaplasia in human airway epithelia. We predicted that the mechanism of action involves TGF-β, ERBB, or EHF, which may act as downstream checkpoints for goblet cell metaplasia, and also suggests that the drug should revert IL-17–induced goblet cell metaplasia. We experimentally confirmed that geldanamycin reverted IL-17–induced goblet cell metaplasia. Taken together, our findings suggest that persistent airway goblet cell metaplasia requires HSP90 activity and that HSP90 inhibitors will revert goblet cell metaplasia, despite active upstream inflammatory signaling. Moreover, HSP90 inhibitors may be a therapeutic option for airway diseases with goblet cell metaplasia of an unknown mechanism of action.

Results

IL-13 induces donor-dependent goblet cell metaplasia in primary cultures of human airway epithelia. To measure variability in the IL-13 response among 12 different donors, primary airway epithelia were cultured from the lungs of the donors, and cells were grown in vitro for 21 days at an air-liquid interface and exposed to 20 ng/ml IL-13. This dosage was used in all experiments. Goblet cells were quantified by diastase periodic acid-Schiff (dPAS) staining and MUC5AC immunofluorescence (Figure 1, A–F), which showed that the IL-13 exposure had no effect on total cell numbers (data not shown) but increased the relative proportion of goblet cells (Figure 1G), findings consistent with goblet cell metaplasia. The magnitude of each donor's IL-13 response was reproducible in many epithelia from the same donor (Supplemental Figure 1; supplemental material available online with this article; https://doi.org/10.1172/JCI123524DS1). In contrast, the response among different donors varied and was not explained by age, sex, or history of smoking (Supplemental Figure 2). We conclude that IL-13 exposure results in an in vitro organotypic experimental model of goblet cell metaplasia.

Goblet cell metaplasia induced by IL-13 in human airway epithelia is long lasting but reversible. Mucus hypersecretion can persist for years, even after the initial trigger is removed (e.g., smoking cessation) (39–41). Since mucus hypersecretion in Th2-high asthma can be alleviated by Th2 pathway blockade (52), we hypothesized that removing IL-13 would alleviate IL-13–induced goblet cell metaplasia. To test this, goblet cell metaplasia was induced in airway epithelia by exposure of the epithelia to IL-13 for 21 days, so that by day 21, goblet cells comprised 16% ± 3.5% of the epithelium. IL-13 exposure was then stopped, and epithelia were examined at 3 later time points (Figure 1H). Ten and twenty-one days after IL-13 discontinuation, we found that 13.3% ± 3.8% and 7.4% ± 2.3% of cells, respectively, were MUC5AC positive. By day 51 after withdrawal of IL-13 (and 72 days after the IL-13 exposure was initiated), MUC5AC-positive cells were absent in cultures from all but 1 donor. In contrast, we observed that continuous exposure to IL-13 further induced MUC5AC-positive cells, which had reached 50.9% ± 10.4% by day 72 of exposure. Importantly, these data show that IL-13–induced MUC5AC accumulation in goblet cells is long lasting but reversible.

The response to IL-13 in vitro partially recapitulates the transcriptional profile of bronchial epithelia from asthmatic patients. To test whether the transcriptional response to IL-13 in vitro mirrors the in vivo asthma transcriptome, we compared the gene expression signatures of airway goblet cell metaplasia in vitro and in vivo. For these studies, we exposed in vitro cultured primary human bronchial epithelia to IL-13 or vehicle and analyzed the transcriptome by microarray. The assay generated a list of gene expression values, which we analyzed along with 2 data sets from the Gene

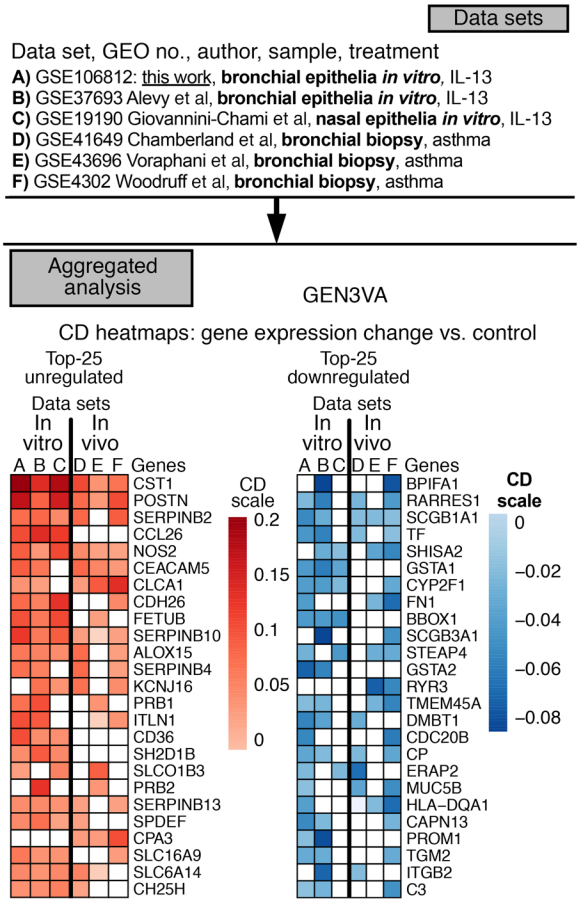

Figure 2. The response to IL-13 in vitro partially recapitulates the in vivo transcriptional profile of asthma in human airway epithelia. A microarray data set of primary human airway epithelia exposed to IL-13 (vs. vehicle) for 21 days (data set A) was generated. Characteristic direction (CD) analysis was performed to facilitate comparisons with other microarray data sets publicly available in the GEO database. A cutoff of the top-500 genes was used for the characteristic direction analysis. Two data sets were derived from bronchial (data set B) and nasal (data set C) epithelia exposed to IL-13 (vs. vehicle) in vitro, and three data sets (data sets D–F) were derived from bronchial biopsies from patients with asthma and their controls. Heatmaps show the top-25 upregulated and downregulated genes compared with controls. Genes are ranked as the sum of characteristic directions from all data sets. Blank squares represent genes that did not pass the 500-gene cutoff for the respective data set. The analysis is publicly available at: amp.pharm.mssm.edu/gen3va/report/497/Pezzulo_IL13.

Expression Omnibus (GEO) that tracked expression in (a) cultured primary human bronchial epithelia exposed to IL-13 for 21 days (45) and (b) primary human nasal epithelia exposed in vitro to IL-13 for 48 hours (53). We compared these expression profiles with in vivo data sets from asthma patients (collected by 3 different research groups; refs. 54–56). Each in vivo data set compared bronchial biopsies from individuals with asthma and their controls (GEO accession numbers are listed in Methods and Figure 2).

To analyze our gene expression data, we chose the characteristic direction method (57) because (a) it is multivariate, accounting for gene-gene statistical dependencies; (b) its magnitude accounts for variance, whereas fold change calculations do not; (c) it outperforms other methods applied to cellular perturbation data; and (d) it facilitates comparisons between data sets. We performed characteristic direction analysis for each data set using the GEO2Enrichr tool (58). The results of this analysis show that many genes were upregulated in response to both IL-13 in vitro and in asthma in vivo (Figure 2). (This information has been uploaded for public access to the GENE Expression and Enrichment Vector Analyzer (GEN3VA) (amp.pharm.mssm.edu/gen3va/report/497/Pezzulo_IL13) (59). Some genes identified were proposed biomarkers of Th2-high asthmatic airway inflammation (60), including periostin (*POSTN*), calcium-activated chloride channel regulator 1 (*CLCA1*) (45, 61), cystatin SN (*CST1*) (62), nitric oxide synthase 2 (*NOS2*), and arachidonate 15-lipoxygenase (*ALOX15*) (26, 63, 64). Downregulated genes (in vitro and in vivo) include secretoglobin family 1A member 1 (*SCGB1A1*, also known as *CC10*), retinoic acid receptor responder 1 (*RARRES1*), transferrin (*TF*), and the WNT signaling antagonist shisa family member 2 (*SHISA2*) (65). Some genes modulated by IL-13 in vitro were not differentially expressed in asthma bronchial biopsies and vice versa (Figure 2).

In our analysis, the transcriptional response of human airway epithelia to IL-13 in vitro was reproducible. Moreover, the transcriptional response to IL-13 in vitro partially recapitulates the transcriptome of airway epithelia from individuals with asthma. This suggests that we may be able to use transcriptome-based strategies, such as perturbation-response connectivity mapping (47–51), to find drugs that may revert goblet cell metaplasia in vivo.

Aggregated analysis of in vivo and in vitro data sets identifies candidate compounds to modulate goblet cell metaplasia. We used perturbation-response connectivity mapping (47–51) to identify candidate compounds for reverting goblet cell metaplasia. Our strategy for each of the in vitro (IL-13–stimulated) or in vivo (asthma) expression profiles (6 data sets total) entailed 4 steps: (a) selecting the set of genes that passed an arbitrary characteristic direction cutoff (>0.03 or ≤0.03); (b) setting the Library of Integrated Network-based Cellular Signatures (LINCS) characteristic direction signature search engine (L1000CDS^2) (66) to the "up" and "down" list mode; (c) entering the gene lists into L1000CDS^2; and (d) obtaining lists of compound signatures that reversed our input.

The output list of L1000CDS^2 can contain multiple entries of the same compound. Each entry shows its effect on a cell line at a specific dose and time point. We assumed that compounds appearing in the output lists multiple times were more likely to induce a cellular response, and so we added the overlap score for all instances of a compound, across all 6 output lists, to generate an aggregated score (Figure 3). Most compounds at the top of the list, including histone deacetylase (HDAC) inhibitors, HSP90 inhibitors, and cyclin-dependent and protein kinase inhibitors, shared mechanisms of action.

Some compound classes were excluded because of potential cytotoxicity. For example, vorinostat and trichostatin A (nonspecific HDAC inhibitors) induced flooding of the in vitro apical compartment and epithelial debridement within 72 hours, and the HDAC inhibitors may have had widespread effects on cellular gene expression at the dose tested. Interestingly, 3 HSP90 inhibitor compounds (geldanamycin, radicicol, and NVP-AUY922) were top candidates, suggesting that pharmacological inhibition of HSP90 may modulate IL-13–induced goblet cell

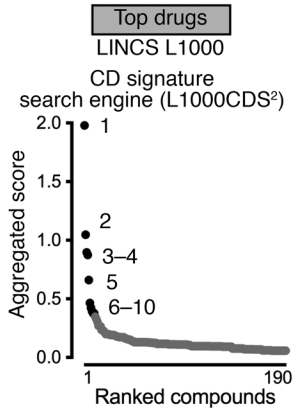

	Compounds	Mechanism of action
1	Vorinostat	HDAC inhibitor
2	Geldanamycin	HSP90 inhibitor
3	CGP-60474	CDK and PKC inhibitor
4	Trichostatin A	HDAC inhibitor
5	Dasatinib	Tyrosine kinases inhibitor
6	Radicicol	HSP90 inhibitor
7	Mitoxantrone	DNA synthesis inhibitor
8	Alvocidib	CDK inhibitor
9	NVP-AUY922	HSP90 inhibitor
10	Curcumin	HDAC inhibitor and others

Figure 3. Aggregated analysis of asthma and IL-13 response transcriptome data sets identifies candidate compounds to modulate goblet cell metaplasia. A list of the top differentially expressed genes based on characteristic direction was generated for each data set included in the study. The lists were analyzed in the LINCS L1000 characteristic direction signature search engine (L1000CDS²). The 6 output lists from L1000CDS² were used to generate an aggregated score for each compound returned. The compounds were ranked from highest to lowest score (graph), and the top 10 are listed.

metaplasia. Unlike nonspecific HDAC inhibitors, geldanamycin did not affect barrier function.

Geldanamycin prevents IL-13–induced goblet cell metaplasia in human airway epithelia in vitro. HSP90 inhibitors (e.g., geldanamycin) were among the top L1000CDS² query candidates for reversion of the IL-13 transcriptional effect on human airway epithelia. We first tested whether HSP90 is modulated during goblet cell metaplasia. We hypothesized that IL-13 would upregulate HSP90 expression. Immunofluorescence confocal microscopy (Figure 4, A–D) revealed that IL-13 induced HSP90 expression in 77.2% ± 3.2% of apical cells (n = 4 biological replicates). Of the HSP90-positive cells detected by immunofluorescence, 55.4% ± 4.1% were goblet cells (based on MUC5AC coexpression). We found that HSP90 was detectable in 100% of goblet cells (Figure 4B). Interestingly, HSP90 expression was low (undetectable in our assay) in ciliated cells (based on acetylated α-tubulin coexpression) after IL-13 stimulation (Figure 4D).

Next, we hypothesized that geldanamycin at the dose ranges tested in the L1000CDS² analysis would prevent IL-13–induced goblet cell metaplasia. Also, since specific HDAC6 inhibitors were recently shown to prevent goblet cell metaplasia (67), we also tested ISOX (a specific HDAC6 inhibitor) (68, 69). Human airway epithelia from multiple donors (n = 4–6) were exposed for 3 weeks to vehicle, IL-13, or IL-13 plus 25 μM geldanamycin (the dosage used for all experiments described here) (Figure 5A). In a second set of studies, epithelial cells were exposed to IL-13 and the HDAC6 inhibitor ISOX (10 μM). Doses of geldanamycin and ISOX were based on the data sets analyzed in L1000CDS².

Our results showed that IL-13 increased the proportion of PAS-positive cells, an effect that was diminished by geldanamycin (Figure 5B). As previously reported, IL-13 exposure reduced the proportion of ciliated cells (70), and our results showed that geldanamycin prevented this effect (Figure 5C). Furthermore, we observed that the HDAC6 inhibitor ISOX caused a dramatic reduction in the total number of cells and an increase in nonciliated/nongoblet cells with decreased epithelial thickness (Figure 5, A, D, and E) at the dose tested. In contrast, the appearance of the HSP90 inhibitor–exposed epithelia was unchanged compared with that of control epithelia. To further test whether HSP90 is involved in IL-13–induced goblet cell metaplasia, we performed dose-response experiments with the benzoquinone ansamycin geldanamycin and its derivative 17-AAG (tanespimycin) (Supplemental Figure 3). We also included a structurally unrelated macrocyclic lactone HSP90 inhibitor (radicicol) (71–73). We found that all of these drugs were able to reduce IL-13–induced goblet cell metaplasia by at least 50%. Previous potency estimates range from low-mid nanomolar to micromolars, suggesting possible cell type– and context-specific potency for HSP90 inhibitors. These results indicate that functional HSP90 may be required for IL-13–induced goblet cell metaplasia. Moreover, HSP90 inhibition may

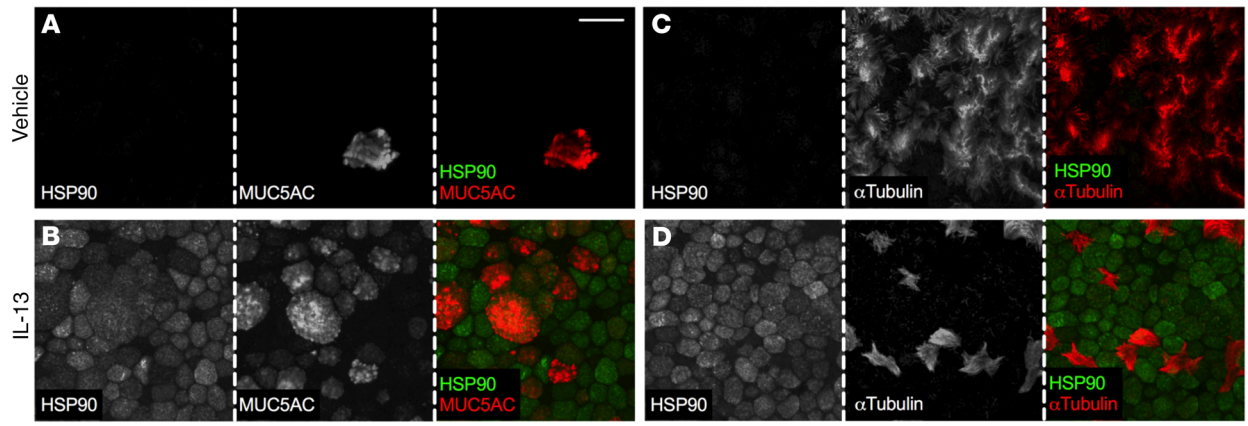

Figure 4. IL-13 induces HSP90 expression. Primary human airway epithelia in vitro were exposed to vehicle (**A** and **C**) or IL-13 (**B** and **D**) for 21 days. Immunofluorescence was performed for HSP90, MUC5AC (goblet cells, **A** and **B**), and acetylated α-tubulin (ciliated cells, **C** and **D**). Scale bar: 20 μm.

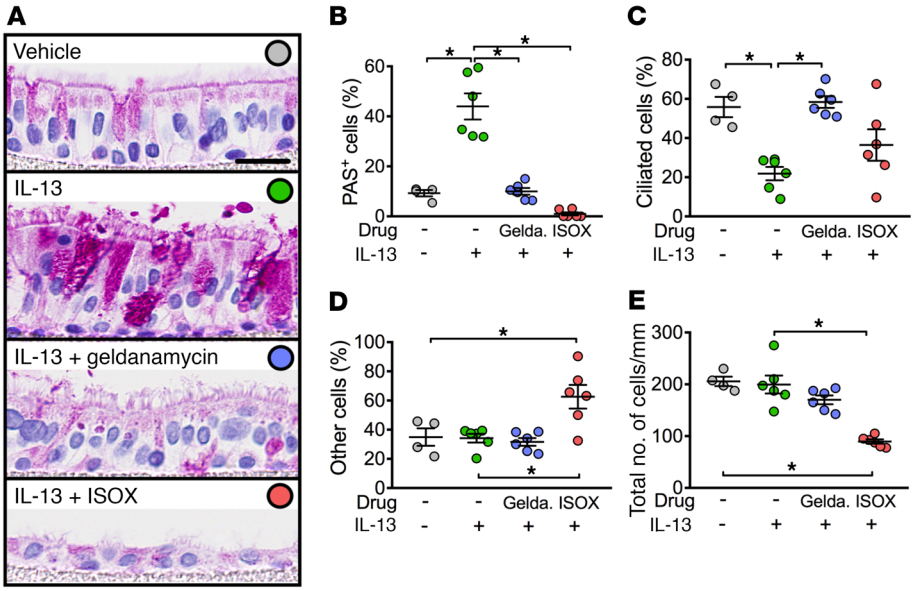

Figure 5. HSP90 inhibition prevents IL-13–induced goblet cell metaplasia in human airway epithelia in vitro. Primary human airway epithelia in vitro were exposed for 21 days to vehicle, IL-13, IL-13 and the HSP90 inhibitor geldanamycin (25 μM), or IL-13 and the HDAC6 inhibitor ISOX (10 μM). dPAS staining was performed to evaluate epithelial morphology (**A**) and to quantify goblet cells (**B**), ciliated cells (**C**), and other nongoblet/nonciliated cells (**D**), shown as a percentage of total cells. Total number of cells shown in (**E**). Scale bar: 20 μm. Each data point corresponds to epithelia from a different donor (n = 4 vehicle biological replicates; n = 6 biological replicates for all other groups). Data represent the mean ± SEM. *P <0.01, by ordinary 1-way ANOVA with Tukey's adjustment.

be used as a therapeutic approach to prevent mucus hypersecretion in patients with a Th2-high endotype.

Geldanamycin reverts IL-13–induced goblet cell metaplasia in human airway epithelia. In our in vitro studies, removal of IL-13 decreased the number of MUC5AC-positive cells (Figure 1H). In a practical sense, however, removal of allergic triggers is difficult, so IL-13 and its receptor complex have been therapeutically targeted, resulting in partial clinical improvement (52, 74, 75).

Since geldanamycin may act downstream of the IL-13 receptor (IL-13R) complex, it hypothetically might revert established goblet cell metaplasia, even when exposure to IL-13 continues. To test this hypothesis, we exposed human airway epithelia to IL-13 for 21 days to generate goblet cells. On day 21, geldanamycin was added to the IL-13 media for another 14 days (Figure 6, A–E). Here, despite the continued IL-13 exposure, we found that the cultures exposed to geldanamycin contained 50% fewer goblet cells. This result matches the effect of IL-13 discontinuation depicted in Figure 1H, which shows a reduction in the percentage of MUC5AC-positive cells from 16% to 7.4% after 21 days. Furthermore, the proportion of ciliated cells was inversely correlated with that of goblet cells. Geldanamycin caused a decrease of roughly 12.5% in the total number of cells. These data show that goblet cell metaplasia is reversible with geldanamycin. It is likely that longer exposure to geldanamycin would further decrease the proportion of goblet cells. The inverse correlation between goblet and ciliated cells suggests a possible transdifferentiation between the 2 cell types. Alternatively, goblet cell metaplasia might be reversed by goblet cell death or inhibition of mucin synthesis.

HSP90 inhibition prevents IL-13–induced airway goblet cell metaplasia in mice in vivo. Our experiments in human airway epithelia in vitro show that HSP90 inhibitors can prevent and revert IL-13–induced goblet cell metaplasia. The environment of airway epithelial cells in vivo differs from air-liquid interface culture conditions in important ways (76). Therefore, we tested the effect of geldanamycin in a well-established mouse model of IL-13–induced goblet cell metaplasia in vivo (77–80) (Figure 7). We found that IL-13 increased the proportion of airways with moderate or high goblet cell abundance and that geldanamycin blocked this effect. This result suggests that HSP90 inhibitors may prevent and revert IL-13–induced goblet cell metaplasia when used as therapy in vivo.

Geldanamycin does not induce goblet cell death. HSP90 can affect cell viability, so geldanamycin might, hypothetically, induce goblet cell death. To evaluate cell death in primary human airway epithelia, we performed propidium iodide (PI) viability assays and cleaved caspase 3 apoptosis immunostaining of primary human airway epithelia. Here, airway epithelia were first exposed to IL-13 for 21 days to induce goblet cell metaplasia and then cultures were exposed to geldanamycin for 2 days.

Our results (Figure 8A) showed that human airway epithelia had few (<1%) apoptotic cells at baseline, confirming previous reports that IL-13 is antiapoptotic (81, 82), and further showed that geldanamycin reverted the apoptosis rate to that of baseline. The proportion of cells affected (<1%) is probably too low to account for the magnitude of goblet cell metaplasia reversal by geldanamycin. A PI cell viability assay provided further support for this result (Figure 8B).

During or after cell death, human airway epithelial cells can leave the epithelial layer in a process called anoikis (83–85), so we performed an anoikis assay to microscopically check for extruded cells (86). We found that no extruded cells were detectable in the geldanamycin-treated human airway epithelia (Figure 8C), supporting the notion that HSP90 inhibition by geldanamycin is unlikely to induce goblet cell death.

Geldanamycin decreases the proportion of secretory cells in human airway epithelia. We investigated whether geldanamycin primarily inhibits mucin synthesis. Mucin synthesis inhibition may turn goblet cells into mucin-free cells with intact secretory machinery. We performed immunostaining for the exocytic machinery protein STXBP1 (referred to herein as MUNC18-1; the murine homolog is Munc18a) (80, 87–89) as a secretory goblet cell marker. MUNC18-1 participates in basal mucin secretion and is expressed in secretory and goblet cells at several-fold-higher levels than in other

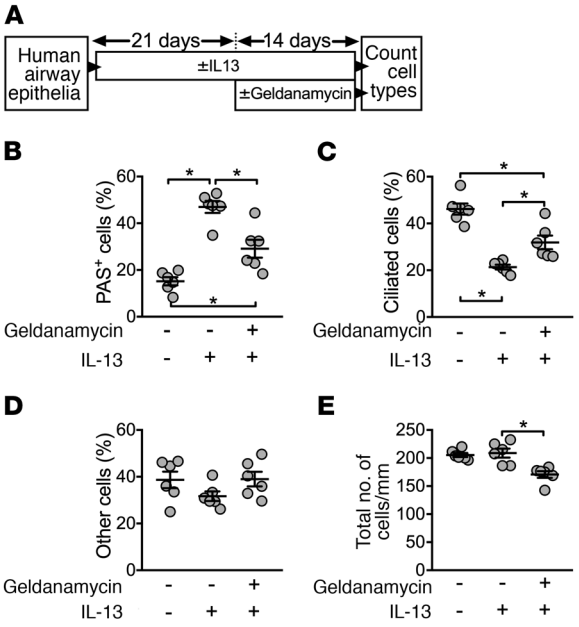

Figure 6. HSP90 inhibition partially reverts IL-13–induced goblet cell metaplasia in human airway epithelia in vitro. Primary human airway epithelia in vitro were exposed to vehicle or IL-13 for 21 days to generate goblet cells in the IL-13 group. Then, while continuing IL-13 exposure, the HSP90 inhibitor geldanamycin was added for 14 days (**A**). dPAS staining was performed to quantify goblet cells (**B**), ciliated cells (**C**), and other nongoblet/nonciliated cells (**D**), shown as a percentage of total cells. Total number of cells shown in (**E**). Each data point corresponds to epithelia from a different donor (n = 6 biological replicates). Data represent the mean ± SEM. *P < 0.05, by Tukey-adjusted ordinary repeated-measures ANOVA with Greenhouse-Geisser correction.

cells (90). The proportion of MUNC18-1–positive cells increased markedly upon IL-13 exposure. Although we expected geldanamycin treatment to reduce MUC5AC staining without affecting MUNC18, we found that it reduced the proportion of MUNC18-1–positive cells (Figure 8D). These data suggest that geldanamycin does not solely inhibit mucin synthesis to revert goblet cell metaplasia. We speculate that geldanamycin induces the replacement of the secretory machinery with ciliated cell components in human airway epithelia.

Geldanamycin does not block receptor-proximal IL-13 signaling. HSP90 interacts with many potential client proteins, and geldanamycin induces ubiquitination and proteasomal degradation of HSP90 clients (91), including those important for IL-13 signaling in cancer cell lines (e.g., JAK/STAT and AKT, refs. 92, 93; IRS, refs. 94, 95; and NOTCH, ref. 96). To test whether geldanamycin would affect gene modulation by IL-13 in airway epithelia, we used quantitative PCR (qPCR) to measure the modulation of 4 genes relevant to goblet cell metaplasia (Figure 8, E–H). This analysis showed that IL-13 upregulated the *SPDEF* transcription factor (77, 97, 98) and the matricellular protein periostin (*POSTN)* (99) in both the absence and presence of geldanamycin. Also, geldanamycin had no effect on the expression of the NOTCH target *HES1* but partially blocked IL-13 modulation of the secreted type 3 cystatin fetuin B (*FETUB)*. These results show that geldanamycin does not affect HSP90-interacting proteins that are involved in IL-13R–proximal signaling, including IL-13R/JAK/STAT and NOTCH.

Geldanamycin affects gene expression in IL-13–stimulated human airway epithelia. Our results suggested that geldanamycin might modulate gene expression downstream of HSP90 clients in human airway epithelia. To test gene expression modulation by geldanamycin, human airway epithelia were exposed to geldanamycin or IL-13 for 2 days. As a control, human airway epithelia were exposed to the HDAC6 inhibitor ISOX. RNA-Seq analysis (Supplemental Table 1) showed that IL-13 modulated 166 genes (threshold $\log_2$ fold change of 2, adjusted $P < 0.1$) (Figure 9A). In comparison, ISOX modulated 1294 genes (Figure 9B). Surprisingly, geldanamycin alone modulated only 5 genes (Figure 9C). These data show that geldanamycin only minimally affects the transcriptome of unstimulated human airway epithelial cells, suggesting that HSP90 activity in these cells is low.

We hypothesized that geldanamycin would affect the expression of IL-13–modulated genes and thus compared human airway epithelia exposed to IL-13 alone and in combination with geldanamycin (Figure 9D). After 2 days, RNA-Seq identified 32 genes as modulated by geldanamycin in IL-13–exposed cells. Most genes followed 3 patterns: (a) they were upregulated by IL-13, and this effect was reverted by geldanamycin (Figure 10A, quadrant IV); (b) they were downregulated by IL-13 and were further downregulated by geldanamycin (Figure 10A, quadrant III); or (c) they were downregulated by IL-13, and geldanamycin reverted the effect (Figure 10A, quadrant I). Our data suggest that, in contrast to unstimulated cells, HSP90 activity increases in IL-13–stimulated airway epithelia.

Geldanamycin affects HSP90 clients important for both IL-13 and IL-17 signaling. The group of IL-13–modulated genes affected by geldanamycin (Figure 10A) might potentially share an upstream regulator. This regulator would likely be the HSP90 client altered by geldanamycin in airway epithelia. To identify upstream regulators for the set of HSP90-affected genes, we used Ingenuity Pathway Analysis (IPA) (QIAGEN; www.qiagenbioinformatics.com/products/ingenuity-pathway-analysis/) (100) (Figure 10B). The top hit predicts that modulation of NCOA3 function by geldanamycin may affect ERBB2, EGFR/ERBB1, PPARG, JNK, ESR1, EHF, and/or TGF-β activity. These proteins potentially modulate HSP90-affected genes in IL-13–stimulated airway epithelia (Supplemental Table 2).

Interestingly, the upstream regulators predicted are not part of canonical IL-13R–proximal signaling but are cellular differentiation genes and may be relevant for goblet cell metaplasia in response to any trigger. EGFR (101), EHF (102, 103), and TGF-β (104, 105) are also involved in IL-17 signaling, and NCOA3 could affect the inflammatory response by interacting with AP-1 and altering cytokine translation (106–108).

Geldanamycin reverts IL-17–induced goblet cell metaplasia. Since IL-17 can drive goblet cell metaplasia in chronic bronchitis, cystic fibrosis, and Th2-low asthma (34), we investigated whether geldanamycin can revert goblet cell metaplasia induced by IL-17. Pathway analysis suggested that geldanamycin would revert IL-17–induced goblet cell metaplasia. To explore this, human airway epithelia were exposed to 20 ng/ml IL-17 for 21 days, followed by 14 days of incubation with IL-17 plus geldanamycin. Cell types were quantified by

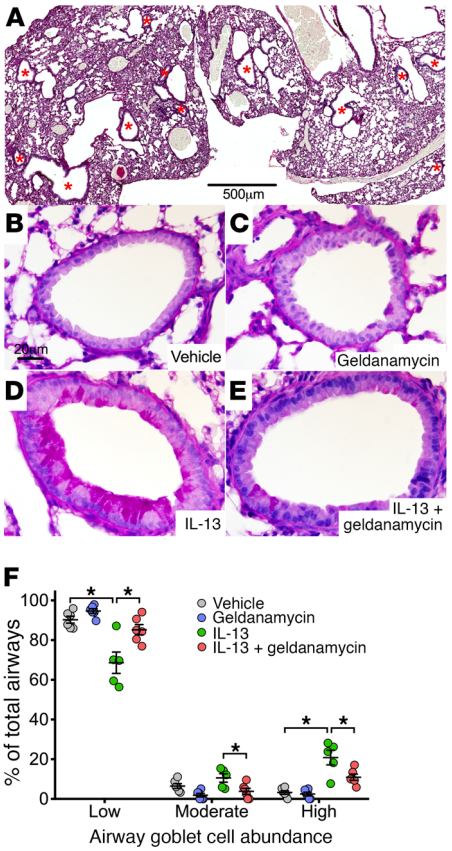

Figure 7. HSP90 inhibition prevents IL-13–induced airway goblet cell metaplasia in mice in vivo. Mice were exposed via intranasal delivery to vehicle, geldanamycin, IL-13 (2.5 μg in 50 μl PBS, 50 μg/ml), or IL-13 plus geldanamycin (25 μM) daily for 4 days. After exposure, lungs were fixed, sectioned and stained with dPAS. Goblet cell abundance was scored for individual airways. (**A**) Images of whole lung sections (red asterisks indicate individual airways). (**B**–**E**) Representative airway images from each treatment group. An average of 40 airways per mouse were scored. (**F**) Goblet cell abundance. Data represent the mean ± SEM (n = 6 mice per group). *$P < 0.05$, by ordinary repeated-measures ANOVA with Tukey's adjustment. Scale bars: 500 μm (**A**) and 20 μm (**B**–**E**).

dPAS staining (Figure 11A), showing that IL-17 alone increased the number of PAS-positive cells in the epithelia (Figure 11B). Moreover, geldanamycin decreased the proportion of PAS-positive cells to baseline levels. Although geldanamycin affected neither the proportion of ciliated cells nor total cell numbers (Figure 11C), we found that it increased the proportion of cells classified as "other" (Figure 11, D and E). These data show that IL-17–induced goblet cell metaplasia is reversible by geldanamycin and that geldanamycin can revert both IL-13– and IL-17–induced goblet cell metaplasia, suggesting that HSP90 inhibitors may control mucus hypersecretion in any asthma endotype as well as in other lung diseases.

Discussion

Here, we identified candidate compounds for human airway chronic mucus hypersecretion therapy. We made use of the transcriptional response of an in vitro organotypic model of IL-13–induced airway goblet cell metaplasia. We combined our data with previously published data sets and used the comparative transcriptomic data in a drug-repurposing approach. As suggested by our analysis, the HSP90 inhibitor geldanamycin prevented the development of goblet cell metaplasia and reverted goblet cell metaplasia that had been caused by exposure to IL-13 and IL-17. Geldanamycin did not kill goblet cells or solely block mucin synthesis but rather affected the expression of genes downstream of proteins essential for cellular differentiation. Moreover, geldanamycin only affected stimulated airway epithelia.

Our approach provided several strengths that may improve the generalizability of our findings to the clinical setting. Primary human airway epithelial cells from many donors were included in our analysis, which showed that the response to both IL-13 and geldanamycin is donor dependent. Also, we collected data from both in vitro and in vivo human cells and used an a priori knowledge–independent connectivity approach to discover novel therapeutic targets (47–51, 66). Finally, we validated the findings and tested further hypotheses in our model system and in an in vivo mouse model of airway goblet cell metaplasia.

Our approach led us to important insights. To our knowledge, our findings have not been reported before, despite existing literature about both goblet cell metaplasia and HSP90. The perturbation-response connectivity analysis pointed to HSP90 inhibitors as goblet cell metaplasia therapy. Surprisingly, although the data used for the connectivity approach included IL-13–stimulated cells, geldanamycin did not affect canonical IL-13R–proximal signaling. Moreover, the effects of HSP90 inhibition in human airway cells became evident only upon exposure to a cytokine. Our analysis predicted that geldanamycin affected signaling by HSP90 clients including ERBB (ERBB1/EGFR and ERBB2-4), TGF, NCOA3/SRC3, and EHF. These targets are relevant in both IL-13– and IL-17–induced goblet cell metaplasia (101–108). Finally, this prediction led us to hypothesize and confirm that geldanamycin would modulate IL-17–driven goblet cell metaplasia.

Th17 and other cells secrete IL-17 in the airways in response to environmental stimuli (reviewed in ref. 109). IL-17, TNF, IL-1, IL-8, and others may drive neutrophilic airway inflammation in chronic bronchitis, cystic fibrosis, viral respiratory infections (110–112), and the Th2-low asthma endotype (31, 34, 113). Th2-low asthma can be severe and corticosteroid resistant, and targeted interventions for Th2-low asthma have been mostly unsuccessful (reviewed in refs. 37, 114). The lack of success of IL-17 or TNF-α blockade (38, 115–118) may be due to disease trigger heterogeneity. Alternatively, goblet cells may be resistant to blockade of a single signaling pathway. Blockade of inflammatory signaling downstream of IL receptors may disrupt goblet cell robustness. Moreover, we showed that IL-17–stimulated epithelia responded to geldanamycin more uniformly than did IL-13–stimulated epithelia. This finding suggests that geldanamycin affects an HSP90 client more important for IL-17 than for IL-13–induced goblet cell metaplasia.

HSP90 is one of the most abundant proteins in both stressed and normal cells (119), and it interacts with many client proteins and participates in steroid hormone receptor and protein kinase signaling (reviewed in refs. 120, 121). HSP90 also interacts with human E3 ubiquitin ligases, transcription factors, and proteins such as NLRs, CFTR, calcineurin, and eNOS. A comprehensive and updated list can be found on the website of the Didier Picard

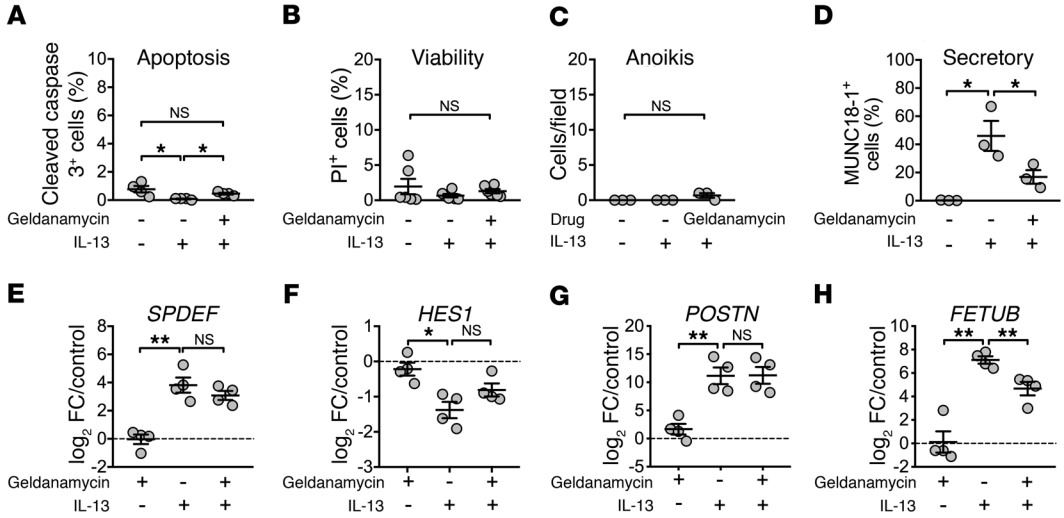

Figure 8. Effects of geldanamycin on human airway epithelia. Geldanamycin did not induce goblet cell death. (**A**–**C**) Primary human airway epithelia in vitro were exposed to vehicle or IL-13 for 21 days to generate goblet cells in the IL-13–treated group. Then, the HSP90 inhibitor geldanamycin was added for 2 days, and cleaved caspase 3 immunostaining (**A**), PI viability staining (**B**), and washing of the apical surface were performed to detect cells extruded from epithelia (anoikis, **C**). (**D**) Geldanamycin did not solely block mucin synthesis. Results of immunostaining for the exocytic machinery component MUNC18-1. Geldanamycin did not affect canonical IL-13 signaling. (**E**–**H**) Primary human airway epithelia in vitro were exposed to vehicle and IL-13 with or without geldanamycin for 2 days. qPCR of the IL-13–STAT6 target *SPDEF* (**E**), the NOTCH target *HES1* (**F**), and the secreted proteins periostin (*POSTN*) (**G**) and fetuin B (*FETUB*) (**H**). Each data point corresponds to epithelia from a different donor. $n = 4$ (**A** and **E**–**H**), $n = 6$ (**B**), and $n = 3$ (**C**–**D**) biological replicates. Data represent the mean ± SEM. $^*P < 0.05$ and $^{**}P < 0.01$ by Tukey-adjusted ordinary repeated-measures ANOVA with Greenhouse-Geisser correction.

Laboratory (https://www.picard.ch/). The main isoforms of HSP90 (reviewed in ref. 122) are HSP90 α ("inducible"), HSP90 β ("constitutive"), the ER isoform GRP94, and HSP75 (also known as TRAP1) in the mitochondrial matrix. HSP90 isoforms vary in regulation and function. Whereas HSP90 α–KO mice are viable, HSP90 β–KO mice die before birth (121, 123, 124). HSP90 α and β have variable affinities for client proteins and small-molecule inhibitors (125). HSP90 has cellular functions beyond those of a protein chaperone, including in signal transduction and pausing of RNA polymerase II (126–129).

Geldanamycin is a benzoquinone ansamycin that inhibits HSP90 by interfering with its ATP-binding site (71, 73), the function of which is essential for HSP90 function in vivo (130). Geldanamycin may affect all 4 main isoforms of HSP90 (122). At high doses, geldanamycin might also affect targets other than HSP90 (131). Our dose-response experiments with 3 different HSP90 inhibitors, including both benzoquinone ansamycins (geldanamycin and 17-AAG) and a macrocyclic lactone (radicicol), indicate that HSP90 and its inhibition play a role in goblet cell metaplasia.

The decrease in goblet cell metaplasia induced by geldanamycin could be caused by isolated inhibition of mucin synthesis, goblet cell death, goblet-to-other-cell-type transdifferentiation, or any combination thereof. Our data suggest that geldanamycin neither solely inhibits mucin synthesis nor causes significant goblet cell death above that observed at baseline.

HSP90 inhibitors selectively kill cancer cells that maintain HSP90 in multichaperone complexes. These complexes have a much higher affinity for inhibitors than do the inactive HSP90 counterparts in normal cells (132). Although HSP90 determines cellular viability in cancer cells, its role is probably different in noncancerous cells. Our data show that, when exposed to HSP90 inhibitors for 3 weeks, human airway epithelia maintain barrier function and normal cellular composition. While we observed a decrease of 12.5% in the total number of cells in the goblet cell metaplasia reversion experiment, neither the apoptosis/viability assays nor the anoikis assay detected significant cell death. It is possible that in certain donors, geldanamycin-induced cell death occurs at a daily rate below the detection level of the assays used in this work. Moreover, at doses higher than those used here, geldanamycin and other HSP90 inhibitors are likely to induce cytotoxicity. Our data suggest that unstimulated, well-differentiated primary airway epithelial cells may not require high HSP90 activity for normal function.

Our data suggest, but do not prove, that geldanamycin induces the transdifferentiation of goblet cells into ciliated or other cell types. In human cells in vitro, IL-13 induces ciliated cells to transdifferentiate into goblet cells (82, 133, 134). In contrast, mouse club cells transdifferentiate into goblet cells in vivo (15, 135–138). Interestingly, heat shock–induced dissociation of HSP90 from cilia leads to cilia resorption (95). Previous reports suggest but do not demonstrate that goblet cells might transdifferentiate into ciliated or other cell types (10, 139).

Clinical trials of HSP90 inhibitors for various diseases are ongoing, and compounds with improved efficacy and side-effect profiles are in active development (reviewed in refs. 71, 140). Our findings point to a promising therapeutic strategy, but the goal of reducing chronic mucus hypersecretion must be approached cautiously. Although chronic mucus hypersecretion is disabling, it may be a predominantly protective response in chronic lung diseases. Therefore, normalization of mucus production could potentially worsen clinical outcomes. While our study showed that geldanamycin affected goblet cell

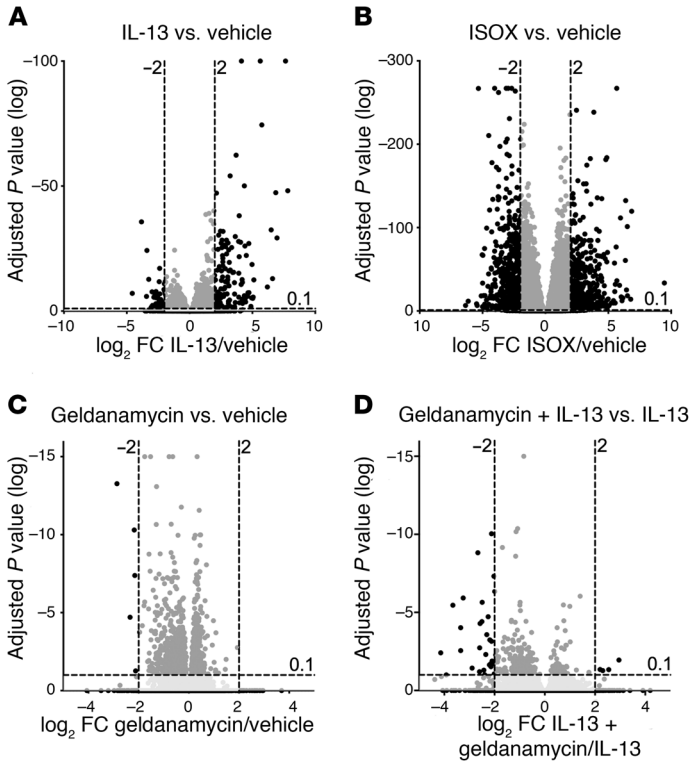

Figure 9. Geldanamycin affects gene expression in human airway epithelia only after IL-13 stimulation. Primary human airway epithelia in vitro were exposed to vehicle or IL-13 (**A**), the HDAC6 inhibitor ISOX (10 μM, positive control) (**B**), or the HSP90 inhibitor geldanamycin without (**C**) or with (**D**) IL-13 for 2 days. RNA-Seq was performed to determine the gene expression profile for each group, and volcano plots are shown. Dashed lines represent arbitrary cutoffs of adjusted $P < 0.05$ or $P < 0.1$ and a $\log_2$ fold change of 2 or less, 2 or greater, or greater than 2. Some extremely small P values were arbitrarily cut to –100(log) to facilitate visualization. Each data point corresponds to a gene. n = airway epithelia from 8 donors. FC, fold change.

metaplasia, some aspects of the IL-13 response, including periostin upregulation, were not affected, which may continue to have detrimental effects on the airways (99). Moreover, it may be important to target specific mucin types to achieve clinical improvement (reviewed in ref. 141).

Goblet cell metaplasia is a significant feature of many chronic lung diseases. We showed that an HSP90 inhibitor, geldanamycin, reverts the goblet cell metaplasia that is induced by exposure to IL-13 and IL-17. HSP90 inhibition reverts goblet cell metaplasia without affecting canonical IL-13 signaling, suggesting novel alternative mechanisms in goblet cell differentiation. Importantly, HSP90 inhibitors may modulate goblet cell metaplasia driven by various mechanisms in chronic lung diseases that currently lack effective therapies.

Methods

Differentiated primary cultures of airway epithelia

Cells were obtained from the University of Iowa Cells and Tissue Core. Epithelial cells were isolated from the trachea and bronchi by enzymatic digestion, seeded onto collagen-coated, semipermeable membranes (0.6 cm^2 Millicell-PCF; MilliporeSigma), and grown at the air–liquid interface as previously described (142). Culture medium, a 1:1 mixture of DMEM/F12, was supplemented with 2% Ultroser G (PALL Corp.). Differentiated epithelial cells were used at least 14 days after seeding. All experiments were performed on passage-0 primary cells obtained from fresh tissue. Media were changed every 2 days. At every media change, 20 μl basolateral media were uniformly added to the apical surface to allow basolateral and apical exposure to treatment conditions. Treatment conditions included IL-13 (20 ng/ml), IL-17 (20 ng/ml), geldanamycin (25 μM), and HDAC6 inhibitor ISOX (10 μM). Treatment durations are indicated in the results section corresponding to each experiment. Reagent details are provided in the Supplemental Methods.

Imaging assays

dPAS staining. dPAS staining was performed on sections of paraformaldehyde-fixed, paraffin-embedded human airway epithelia.

Immunofluorescence. Reagent details, including antibody catalog and lot numbers, are provided in the Supplemental Methods. Primary human airway epithelial cultures were gently washed with PBS (Thermo Fisher Scientific), fixed with 4% paraformaldehyde (Electron Microscopy Sciences) in PBS for 15 minutes, permeabilized with 0.3% Triton-X (Thermo Fisher Scientific) in PBS for 20 minutes, blocked with 2% BSA (Research Products International) in SuperBlock (Thermo Fisher Scientific) for 1 hour at room temperature, incubated with

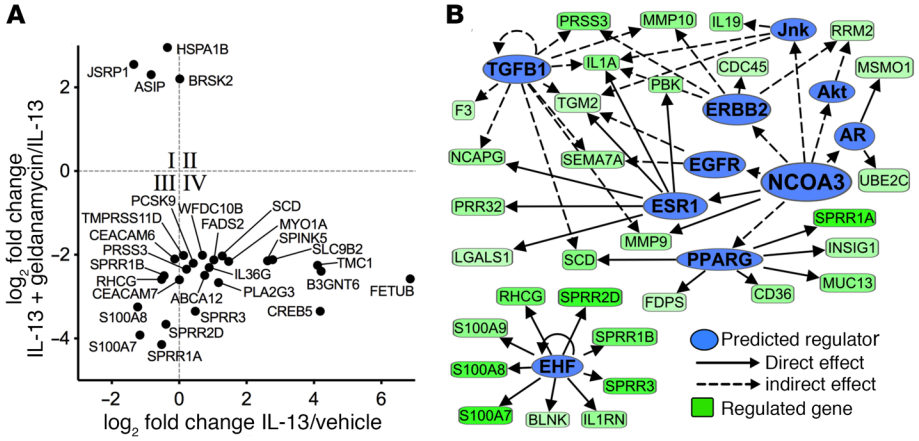

Figure 10. Geldanamycin blocks the modulation of pathways relevant for both IL-13– and IL-17–induced goblet cell metaplasia. Differential regulation scatter plot (**A**) of data from Figure 7D. Genes for which modulation by IL-13 was affected at by least 1-fold ($\log_2$) are shown. (**B**) IPA-predicted causal network (NCOA3) and upstream regulators for genes downmodulated by geldanamycin.

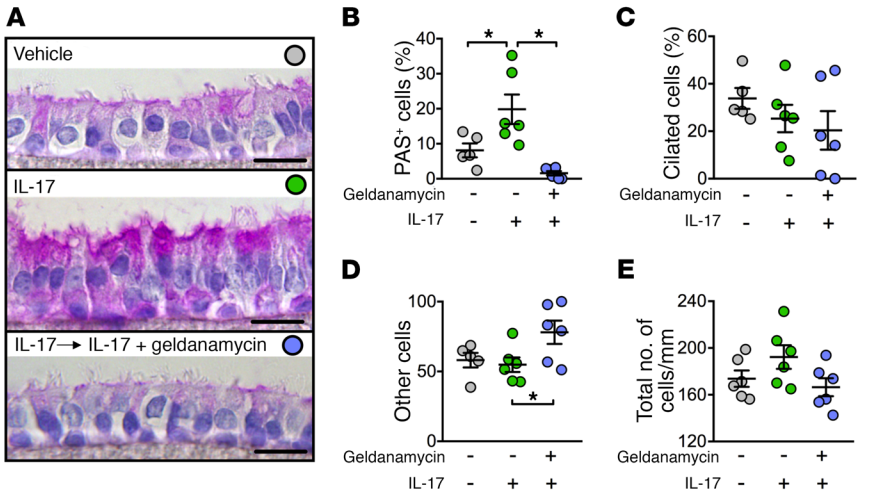

Figure 11. HSP90 inhibition reverts IL-17–induced goblet cell metaplasia. Primary human airway epithelia in vitro were exposed to vehicle or 20 ng/ml IL-17 for 21 days to generate goblet cells in the IL-17 group. Then, while continuing IL-17 exposure, the HSP90 inhibitor geldanamycin was added for 14 days. (**A**) dPAS staining was performed to quantify goblet cells (**B**), ciliated cells (**C**), and other non-goblet/nonciliated cells (**D**), shown as a percentage of total cells. Total number of cells shown in (**E**). Each data point corresponds to epithelia from a different donor (n = 6 biological replicates). Data represent the mean ± SEM. *P < 0.05, by Tukey-adjusted ordinary repeated-measures ANOVA with Greenhouse-Geisser correction. Scale bar: 20 μm.

primary antibody apically for 1.5 hours at 37°C, and then incubated with the appropriate secondary antibody for 1 hour at 37°C, both diluted in 2% BSA and SuperBlock. Samples were probed with the following primary antibodies: mouse anti-MUC5AC (1:5000; Thermo Fisher Scientific), rabbit antiacetylated α-tubulin (1:300; Cell Signaling Technology), rabbit anti–cleaved caspase 3 (1:100; Cell Signaling Technology), and rabbit anti-STXBP1/MUNC18-1 (1:100; Bioss, purchased through Sapphire Biosciences). The secondary antibodies used were goat anti-rabbit and goat anti-mouse conjugated to Alexa Fluor 488 or 568 (1:1000; Thermo Fisher Scientific). To examine localization of MUC5AC relative to the cortical cytoskeleton enriched right beneath the apical cell membrane, we also used the actin stain phalloidin (1:40; Thermo Fisher Scientific) after secondary antibody incubation. For assessment of cell membrane viability, cells were washed with PBS and then stained with PI (Thermo Fisher Scientific) for 15 minutes under light-shielded conditions. After immunostaining, the cultures were mounted on Superfrost Plus Microscope Slides (Thermo Fisher Scientific) in Vectashield with DAPI (Vector Laboratories) and then coverslipped.

For the anoikis assay, cells were washed apically with PBS before treatment with geldanamycin. PBS was used as a negative control. EGTA (8 mM; Research Products International) was used as a positive control (data not shown). After treatment, apical washes were collected and loaded into a cytospin apparatus. Samples were spun into glass slides at 800 rpm for 5 minutes and then soaked in methanol for 20 minutes, washed with PBS, mounted in Vectashield with DAPI, and coverslipped. All immunofluorescence studies were performed using an Olympus FluoView FV1000 confocal microscope with a UPLSAPO ×60 oil lens, and all confocal images were processed using the Olympus FluoView program.

Quantification of cell types. To analyze the airway epithelial architecture and quantify cell type composition, we used the Cell Counter plugin within the Fiji distribution of ImageJ software (NIH) (143, 144). A single group-blinded reader examined images of the dPAS-stained cultures and used a standardized linear distance to manually select and classify cell types. Cells with cilia visible on the apical surface were classified as ciliated cells, cells with PAS-positive staining were classified as goblet cells, and nonciliated and nongoblet cells were classified as other types. For each sample, a total of 6 images from different areas of the filters were used, and the counts were averaged.

Quantification of confocal images. TIFF files were formatted from Z-stacks of the original confocal images. The number of cells positive for MUC5AC, PI, cleaved caspase 3, or STXBP1/MUNC18-1 was manually counted. For the anoikis assays, the number of whole nuclei detected by DAPI was counted. For each sample, a total of 4 random images were taken, 1 from each quadrant, and the counts were averaged.

In vivo mouse model

Six- to eight-week-old C57BL/6NHsd male mice (Envigo) were anesthetized with isoflurane and then exposed (via intranasal pipette delivery) to vehicle, geldanamycin, IL-13 (2.5 μg in 50 μl PBS, 50 μg/ml), or IL-13 plus geldanamycin (25 μM) daily for 4 days. According to Pope et al. and Mishra et al. (78, 145), approximately 70% of the instilled volume is aspirated into the lungs. On day 5, lungs were collected and fixed, uninflated, with 2 ml 10% NBF perfusion via the pulmonary circulation and stored in 10% neutral-buffered formalin (NBF) at 4°C for 4 days. Lungs were paraffin embedded in a configuration that allowed for sections through all lobes. Whole-lung sections were used for dPAS staining, and the slides were imaged with an Ariol Slide-Scanning Microscope (Leica Biosystems). An average of 40 airways were scored per mouse. The airway goblet cell abundance score was based on the percentage of surface composed of goblet cells and classified as follows: low = less than 25%; moderate = 25%–50%; and high = greater than 50%. Inter-rater reliability (146) was evaluated in a fully crossed, blinded manner by 3 different raters. The R package "irr," version 0.84 (147–149) was used, and a Light's κ (150) of 0.858 was calculated. Data reported are from a single rater on a full data set.

Gene expression microarray sample processing

TRIzol (15596018, Life Technologies, Thermo Fisher Scientific) extraction of total RNA from human airway epithelia was performed according to the manufacturer's instructions. Microarray sample processing was performed as detailed in the Supplemental Methods. Arrays were scanned with the Affymetrix Model 3000 scanner with a 7G upgrade, and data were collected using GeneChip Operating Software (GCOS), version 1.4. The data were imported into Partek Genomics Suite, version 6.15.0327, to perform robust multiarray average (RMA) with background subtraction, quantile normalization, and

log_2 transformation. Data were uploaded to the NCBI's GEO database (GEO GSE106812) (151, 152).

Microarray data analysis and GEO data reanalysis

We analyzed the following data sets (labeled here and in Figure 2 as data sets A–F) from the NCBI's GEO database: (A) GSE106812 (Pezzulo_Bronchial_IL-13, in vitro, from this article); (B) GSE37693 (Alevy_Bronchial_IL-13, in vitro) (45); (C) GSE19190 (Giovannini-Chami/Barbry_Nasal_IL-13, in vitro) (53); (D) GSE41649 (Chamberland_Bronchial_Asthma, in vivo) (54); (E) GSE43696 (Voraphani_Bronchial_Asthma, in vivo) (55); and (F) GSE4302 (Woodruff_Bronchial_Asthma, in vivo) (56).

Data were uploaded from the GEO database into GEO2Enrichr (58). Incompatible GEO data sets were downloaded and formatted for manual entry into GEO2Enrichr. Characteristic direction analysis (57)was run for each data set, with a 500-gene cutoff. For each GEO-2Enrichr run, the tag "Pezzulo_IL-13" was included for automatic meta-analysis in GEN3VA (59). The GEN3VA report and data used for this analysis are available at http://amp.pharm.mssm.edu/gen3va/report/497/Pezzulo_IL13. The report contains links to each of the 6 GEO2Enrichr data sets.

LINCS CDS2 and overlap score

For each 1 of the 6 data sets, genes passing a characteristic direction cutoff of 0.03 for up- and downregulated genes were entered into the LINCS Characteristic Direction Signature Search Engine ($L1000CDS^2$) (66). $L1000CDS^2$ was set to the "up" and "down" list mode. The 6 resulting tables were concatenated. An aggregated overlap score was generating by the addition of overlap scores when summarizing the data per compound.

RNA-Seq

RNA-Seq data are available in the NCBI's GEO database (GEO GSE116927).

RNA from primary human airway epithelia was isolated with the RNeasy Lipid Tissue Mini Kit (QIAGEN). Two cultures (approximately 600,000 cells total) were used for each extraction. Initial quality control was performed with a NanoDrop 2000 (Thermo Fisher Scientific) and an Agilent Bioanalyzer 2100. Further processing and initial data analysis were performed at the Genomic Division of the Iowa Institute of Human Genetics (Iowa City, Iowa, USA). Sequencing libraries were prepared with the Illumina TruSeq Stranded Total RNA Ribo-Zero Gold Sample Preparation Kit, starting with 500 ng input total RNA and following the Illumina sample preparation guide. The libraries were analyzed on the Fragment Analyzer (Advanced Analytical) and combined into pools at equimolar concentrations. The pools were analyzed on the Agilent 2100 Bioanalyzer using the high-sensitivity chip to evaluate size distribution. The concentration of each pool was measured using the KAPA Illumina Library Quantification Kit (KAPA Biosystems). Pools were sequenced on the Illumina HiSeq 4000 across 3 lanes with 150-bp Paired-End SBS Chemistry.

Raw reads obtained from the sequencer were processed with Kallisto, version 0.44.0 (153), with an index from reference cDNA Ensembl release 91, GRCh38. Noncoding RNA sequences were not analyzed. Each sample was run with 75 bootstraps. Differential expression analysis for transcript-level analysis was performed with Sleuth, version 0.29.0 (154). Additionally, tximport, version 1.3.4 (155), was used to summarize the Kallisto output into gene-level estimates for DESeq2, version 1.18, analysis (156) in R, version 3.4.3, and Bioconductor, version 3.5 (147, 148).

qPCR

Total RNA was extracted from human airway epithelia using the RNeasy Lipid Tissue Mini Kit (QIAGEN). For cDNA synthesis, total RNA was reverse transcribed with SuperScript IV VILO (Invitrogen, Thermo Fisher Scientific) reagents using a standard protocol and run in a SimpliAmp thermocycler (Applied Biosystems). Each SYBR green–based qPCR reaction consisted of a total volume of 20 μl containing SYBR Premix Ex Taq II (TIi RNaseH Plus) Master Mix (Takara), PCR forward primer (0.4 μM), PCR reverse primer (0.4 μM), and 1 μl cDNA template. TaqMan assays were performed using standard Applied Biosystems reagents and protocols. The following primers from Integrated DNA Technologies were used: *SPDEF* (157) (forward: 5′-GTCCGCCTTCTACCTCTCCT-3′; reverse: 5′- GGACTGCACCTGCTCCAG-3′); *POSTN* (158) (forward: 5′-TGCCCAGCAGTTTTGCCCAT-3′; reverse: 5′-CGTTGCTCTCCAAACCTCTA-3′); *FETUB* (forward: 5′-CCATGTGCTCAGAAAGAAGGC-3′; reverse: 5′-ACTGGGCGAAGAGTACAGTTA-3′); *HES1* TaqMan assay hs00172878_m1 (Applied Biosystems) and *ACTB* (159) (forward: 5′-CTGGAACGGTGAAGGTGACA-3′; reverse: 5′-AAGGGACTTCCTGTAACAATGCA-3′). *ACTB* was used as the housekeeping gene. qPCR was performed in 384-well plates, with samples run in triplicate in a QuantStudio 6 Flex Real-Time PCR System (Applied Biosystems). The PCR thermal cycle protocol consisted of the following: 1 cycle of 95°C for 30 seconds, 40 cycles of 95°C for 5 seconds, and 60°C for 30 seconds, ending with 1 cycle of 95°C for 15 seconds, 60°C for 60 seconds, and 95°C for 15 seconds. Expression values were normalized to the housekeeping gene.

IPA

Upstream regulator and causal network analysis was done using IPA (QIAGEN; www.qiagenbioinformatics.com/products/ingenuity-pathway-analysis/), with the confidence level set to experimentally observed only. Genes included passed a threshold of an adjusted *P* value of less than 0.01 and a log_2 fold change of greater than 1 between the IL-13 plus geldanamycin and IL-13 groups. Upstream regulators were sorted according to the predicted activation *Z* score. The causal network analysis data table is available in the Supplemental Table 2.

Statistics

Statistical tests, including 2-tailed paired *t* tests, ordinary 1-way ANOVA with Tukey's adjustment, and repeated-measures ANOVA with Greenhouse-Geisser correction, were performed with GraphPad Prism 7 (GraphPad Software) (160). A *P* value of less than 0.05 was set as the threshold for statistical significance. Analysis of high-throughput data is described above.

Study approval

Animal studies were approved by the IACUC of the University of Iowa.

Author contributions

AP and JZ were responsible for the overall design of the study and wrote the manuscript. AP, RT, CS, BL, PT, NG, and LV performed

experiments. AP and CS were responsible for the high-throughput sample preparation and data analysis.

Acknowledgments

This work was supported by the Parker B. Francis Fellowship Program (to AP) and NHLBI HL051670 and HL091842 (to JZ). We would like to thank Lynda S. Ostedgaard, Michael J. Welsh, David A. Stoltz, Paul B. McCray Jr., David K. Meyerholz (University of Iowa), and Burton F. Dickey (MD Anderson Cancer Center) for their helpful discussions.

Address correspondence to: Joseph Zabner, Department of Internal Medicine, Roy J. and Lucille A. Carver College of Medicine, 6324 PBDB; 169 Newton Road, Iowa City, Iowa 52242, USA. Phone: 319.335.8475; E-mail: joseph-zabner@uiowa.edu.

1. Evans CM, Koo JS. Airway mucus: the good, the bad, the sticky. *Pharmacol Ther*. 2009;121(3):332–348.
2. Kreda SM, Davis CW, Rose MC. CFTR, mucins, and mucus obstruction in cystic fibrosis. *Cold Spring Harb Perspect Med*. 2012;2(9):a009589.
3. Vestbo J, Prescott E, Lange P. Association of chronic mucus hypersecretion with FEV1 decline and chronic obstructive pulmonary disease morbidity. Copenhagen City Heart Study Group. *Am J Respir Crit Care Med*. 1996;153(5):1530–1535.
4. Boucherat O, Boczkowski J, Jeannotte L, Delacourt C. Cellular and molecular mechanisms of goblet cell metaplasia in the respiratory airways. *Exp Lung Res*. 2013;39(4-5):207–216.
5. Ordoñez CL, et al. Mild and moderate asthma is associated with airway goblet cell hyperplasia and abnormalities in mucin gene expression. *Am J Respir Crit Care Med*. 2001;163(2):517–523.
6. Wills-Karp M, et al. Interleukin-13: central mediator of allergic asthma. *Science*. 1998;282(5397):2258–2261.
7. Atherton HC, Jones G, Danahay H. IL-13–induced changes in the goblet cell density of human bronchial epithelial cell cultures: MAP kinase and phosphatidylinositol 3-kinase regulation. *Am J Physiol Lung Cell Mol Physiol*. 2003;285(3):L730–L739.
8. Grünig G, et al. Requirement for IL-13 independently of IL-4 in experimental asthma. *Science*. 1998;282(5397):2261–2263.
9. Jiang H, Harris MB, Rothman P. IL-4/IL-13 signaling beyond JAK/STAT. *J Allergy Clin Immunol*. 2000;105(6 Pt 1):1063–1070.
10. Kondo M, et al. Elimination of IL-13 reverses established goblet cell metaplasia into ciliated epithelia in airway epithelial cell culture. *Allergol Int*. 2006;55(3):329–336.
11. Gour N, Wills-Karp M. IL-4 and IL-13 signaling in allergic airway disease. *Cytokine*. 2015;75(1):68–78.
12. Guseh JS, et al. Notch signaling promotes airway mucous metaplasia and inhibits alveolar development. *Development*. 2009;136(10):1751–1759.
13. Morimoto M, Liu Z, Cheng HT, Winters N, Bader D, Kopan R. Canonical Notch signaling in the developing lung is required for determination of arterial smooth muscle cells and selection of Clara versus ciliated cell fate. *J Cell Sci*. 2010;123(Pt 2):213–224.
14. Morimoto M, Nishinakamura R, Saga Y, Kopan R. Different assemblies of Notch receptors coordinate the distribution of the major bronchial Clara, ciliated and neuroendocrine cells. *Development*. 2012;139(23):4365–4373.
15. Pardo-Saganta A, Law BM, Gonzalez-Celeiro M, Vinarsky V, Rajagopal J. Ciliated cells of pseudostratified airway epithelium do not become mucous cells after ovalbumin challenge. *Am J Respir Cell Mol Biol*. 2013;48(3):364–373.
16. Pardo-Saganta A, et al. Parent stem cells can serve as niches for their daughter cells. *Nature*. 2015;523(7562):597–601.
17. Rock JR, Gao X, Xue Y, Randell SH, Kong YY, Hogan BL. Notch-dependent differentiation of adult airway basal stem cells. *Cell Stem Cell*. 2011;8(6):639–648.
18. Tsao PN, Vasconcelos M, Izvolsky KI, Qian J, Lu J, Cardoso WV. Notch signaling controls the balance of ciliated and secretory cell fates in developing airways. *Development*. 2009;136(13):2297–2307.
19. Chen Y, Thai P, Zhao YH, Ho YS, DeSouza MM, Wu R. Stimulation of airway mucin gene expression by interleukin (IL)-17 through IL-6 paracrine/autocrine loop. *J Biol Chem*. 2003;278(19):17036–17043.
20. Fogli LK, et al. T cell-derived IL-17 mediates epithelial changes in the airway and drives pulmonary neutrophilia. *J Immunol*. 2013;191(6):3100–3111.
21. Fujisawa T, et al. NF-κB mediates IL-1β- and IL-17A-induced MUC5B expression in airway epithelial cells. *Am J Respir Cell Mol Biol*. 2011;45(2):246–252.
22. Zhao J, Lloyd CM, Noble A. Th17 responses in chronic allergic airway inflammation abrogate regulatory T-cell-mediated tolerance and contribute to airway remodeling. *Mucosal Immunol*. 2013;6(2):335–346.
23. Gaffen SL. Structure and signalling in the IL-17 receptor family. *Nat Rev Immunol*. 2009;9(8):556–567.
24. Onishi RM, Gaffen SL. Interleukin-17 and its target genes: mechanisms of interleukin-17 function in disease. *Immunology*. 2010;129(3):311–321.
25. Takeyama K, et al. Epidermal growth factor system regulates mucin production in airways. *Proc Natl Acad Sci U S A*. 1999;96(6):3081–3086.
26. Zhen G, et al. IL-13 and epidermal growth factor receptor have critical but distinct roles in epithelial cell mucin production. *Am J Respir Cell Mol Biol*. 2007;36(2):244–253.
27. Choy DF, et al. TH2 and TH17 inflammatory pathways are reciprocally regulated in asthma. *Sci Transl Med*. 2015;7(301):301ra129.
28. Hall SL, et al. IL-17A enhances IL-13 activity by enhancing IL-13–induced signal transducer and activator of transcription 6 activation. *J Allergy Clin Immunol*. 2017;139(2):462–471.e14.
29. Gallelli L, Busceti MT, Vatrella A, Maselli R, Pelaia G. Update on anticytokine treatment for asthma. *Biomed Res Int*. 2013;2013:104315.
30. Pelaia G, et al. Cellular mechanisms underlying eosinophilic and neutrophilic airway inflammation in asthma. *Mediators Inflamm*. 2015;2015:879783.
31. Trejo Bittar HE, Yousem SA, Wenzel SE. Pathobiology of severe asthma. *Annu Rev Pathol*. 2015;10:511–545.
32. Ray A, Raundhal M, Oriss TB, Ray P, Wenzel SE. Current concepts of severe asthma. *J Clin Invest*. 2016;126(7):2394–2403.
33. Desai M, Oppenheimer J. Elucidating asthma phenotypes and endotypes: progress towards personalized medicine. *Ann Allergy Asthma Immunol*. 2016;116(5):394–401.
34. Svenningsen S, Nair P. Asthma endotypes and an overview of targeted therapy for asthma. *Front Med (Lausanne)*. 2017;4:158.
35. Wesolowska-Andersen A, Seibold MA. Airway molecular endotypes of asthma: dissecting the heterogeneity. *Curr Opin Allergy Clin Immunol*. 2015;15(2):163–168.
36. Douwes J, Gibson P, Pekkanen J, Pearce N. Non-eosinophilic asthma: importance and possible mechanisms. *Thorax*. 2002;57(7):643–648.
37. Diver S, Russell RJ, Brightling CE. New and emerging drug treatments for severe asthma. *Clin Exp Allergy*. 2018;48(3):241–252.
38. Busse WW, et al. Randomized, double-blind, placebo-controlled study of brodalumab, a human anti-IL-17 receptor monoclonal antibody, in moderate to severe asthma. *Am J Respir Crit Care Med*. 2013;188(11):1294–1302.
39. Braman SS. Postinfectious cough: ACCP evidence-based clinical practice guidelines. *Chest*. 2006;129(1 Suppl):138S–146S.
40. Wang K, et al. Montelukast for postinfectious cough in adults: a double-blind randomised placebo-controlled trial. *Lancet Respir Med*. 2014;2(1):35–43.
41. Turato G, et al. Effect of smoking cessation on airway inflammation in chronic bronchitis. *Am J Respir Crit Care Med*. 1995;152(4 Pt 1):1262–1267.
42. Nicodemus-Johnson J, et al. DNA methylation in lung cells is associated with asthma endotypes and genetic risk. *JCI Insight*. 2016;1(20):e90151.
43. Nicodemus-Johnson J, et al. Genome-wide methylation study identifies an IL-13–induced epigenetic signature in asthmatic airways. *Am J Respir Crit Care Med*. 2016;193(4):376–385.
44. Lachowicz-Scroggins ME, et al. Corticosteroid and long-acting ß-agonist therapy reduces epithelial goblet cell metaplasia. *Clin Exp Allergy*. 2017;47(12):1534–1545.
45. Alevy YG, et al. IL-13–induced airway mucus production is attenuated by MAPK13 inhibition. *J Clin Invest*. 2012;122(12):4555–4568.
46. Rogers DF, Barnes PJ. Treatment of airway mucus hypersecretion. *Ann Med*. 2006;38(2):116–125.
47. Kunkel SD, et al. mRNA expression signatures of

human skeletal muscle atrophy identify a natural compound that increases muscle mass. *Cell Metab*. 2011;13(6):627–638.
48. Kunkel SD, et al. Ursolic acid increases skeletal muscle and brown fat and decreases diet-induced obesity, glucose intolerance and fatty liver disease. *PLoS ONE*. 2012;7(6):e39332.
49. Lamb J, et al. The Connectivity Map: using gene-expression signatures to connect small molecules, genes, and disease. *Science*. 2006;313(5795):1929–1935.
50. Campbell JD, et al. A gene expression signature of emphysema-related lung destruction and its reversal by the tripeptide GHK. *Genome Med*. 2012;4(8):67.
51. Hodos RA, Kidd BA, Shameer K, Readhead BP, Dudley JT. In silico methods for drug repurposing and pharmacology. *Wiley Interdiscip Rev Syst Biol Med*. 2016;8(3):186–210.
52. Corren J, et al. Lebrikizumab treatment in adults with asthma. *N Engl J Med*. 2011;365(12):1088–1098.
53. Giovannini-Chami L, et al. Distinct epithelial gene expression phenotypes in childhood respiratory allergy. *Eur Respir J*. 2012;39(5):1197–1205.
54. Chamberland A, Madore AM, Tremblay K, Laviolette M, Laprise C. A comparison of two sets of microarray experiments to define allergic asthma expression pattern. *Exp Lung Res*. 2009;35(5):399–410.
55. Voraphani N, et al. An airway epithelial iNOS-DUOX2-thyroid peroxidase metabolome drives Th1/Th2 nitrative stress in human severe asthma. *Mucosal Immunol*. 2014;7(5):1175–1185.
56. Woodruff PG, et al. Genome-wide profiling identifies epithelial cell genes associated with asthma and with treatment response to corticosteroids. *Proc Natl Acad Sci U S A*. 2007;104(40):15858–15863.
57. Clark NR, et al. The characteristic direction: a geometrical approach to identify differentially expressed genes. *BMC Bioinformatics*. 2014;15:79.
58. Gundersen GW, et al. GEO2Enrichr: browser extension and server app to extract gene sets from GEO and analyze them for biological functions. *Bioinformatics*. 2015;31(18):3060–3062.
59. Gundersen GW, et al. GEN3VA: aggregation and analysis of gene expression signatures from related studies. *BMC Bioinformatics*. 2016;17(1):461.
60. Wesolowska-Andersen A, et al. Dual RNA-seq reveals viral infections in asthmatic children without respiratory illness which are associated with changes in the airway transcriptome. *Genome Biol*. 2017;18(1):12.
61. Sala-Rabanal M, Yurtsever Z, Nichols CG, Brett TJ. Secreted CLCA1 modulates TMEM16A to activate Ca(2+)-dependent chloride currents in human cells. *Elife*. 2015;4:05875.
62. Moheimani F, et al. The genetic and epigenetic landscapes of the epithelium in asthma. *Respir Res*. 2016;17(1):119.
63. Tang X, et al. Foxa2 regulates leukotrienes to inhibit Th2-mediated pulmonary inflammation. *Am J Respir Cell Mol Biol*. 2013;49(6):960–970.
64. Zhao J, O'Donnell VB, Balzar S, St Croix CM, Trudeau JB, Wenzel SE. 15-Lipoxygenase 1 interacts with phosphatidylethanolamine-binding protein to regulate MAPK signaling in human airway epithelial cells. *Proc Natl Acad Sci U S A*. 2011;108(34):14246–14251.
65. Cruciat CM, Niehrs C. Secreted and transmembrane wnt inhibitors and activators. *Cold Spring Harb Perspect Biol*. 2013;5(3):a015081.
66. Duan Q, et al. L1000CDS2: LINCS L1000 characteristic direction signatures search engine. *NPJ Syst Biol Appl*. 2016;2:2016.
67. Ren Y, et al. Therapeutic effects of histone deacetylase inhibitors in a murine asthma model. *Inflamm Res*. 2016;65(12):995–1008.
68. Butler KV, Kalin J, Brochier C, Vistoli G, Langley B, Kozikowski AP. Rational design and simple chemistry yield a superior, neuroprotective HDAC6 inhibitor, tubastatin A. *J Am Chem Soc*. 2010;132(31):10842–10846.
69. Kozikowski AP, Tapadar S, Luchini DN, Kim KH, Billadeau DD. Use of the nitrile oxide cycloaddition (NOC) reaction for molecular probe generation: a new class of enzyme selective histone deacetylase inhibitors (HDACIs) showing picomolar activity at HDAC6. *J Med Chem*. 2008;51(15):4370–4373.
70. Parker JC, et al. Chronic IL9 and IL-13 exposure leads to an altered differentiation of ciliated cells in a well-differentiated paediatric bronchial epithelial cell model. *PLoS ONE*. 2013;8(5):e61023.
71. Kitson RR, Moody CJ. Learning from nature: advances in geldanamycin- and radicicol-based inhibitors of Hsp90. *J Org Chem*. 2013;78(11):5117–5141.
72. Ozgur A, Tutar Y. Heat Shock Protein 90 Inhibitors in Oncology. *Curr Proteomics*. 2014;11(1):2–16.
73. Özgür A, Tutar Y. Heat shock protein 90 inhibition in cancer drug discovery: from chemistry to futural clinical applications. *Anticancer Agents Med Chem*. 2016;16(3):280–290.
74. Choy DF, et al. Peripheral blood gene expression predicts clinical benefit from anti-IL-13 in asthma. *J Allergy Clin Immunol*. 2016;138(4):1230–1233.e8.
75. Shaughnessy AF. Monoclonal antibodies: magic bullets with a hefty price tag. *BMJ*. 2012;345:e8346.
76. Pezzulo AA, et al. The air-liquid interface and use of primary cell cultures are important to recapitulate the transcriptional profile of in vivo airway epithelia. *Am J Physiol Lung Cell Mol Physiol*. 2011;300(1):L25–L31.
77. Park KS, et al. SPDEF regulates goblet cell hyperplasia in the airway epithelium. *J Clin Invest*. 2007;117(4):978–988.
78. Pope SM, et al. IL-13 induces eosinophil recruitment into the lung by an IL-5- and eotaxin-dependent mechanism. *J Allergy Clin Immunol*. 2001;108(4):594–601.
79. Yang M, et al. Interleukin-13 mediates airways hyperreactivity through the IL-4 receptor-alpha chain and STAT-6 independently of IL-5 and eotaxin. *Am J Respir Cell Mol Biol*. 2001;25(4):522–530.
80. Zhu Y, et al. Baseline goblet cell Mucin secretion in the airways exceeds stimulated secretion over extended time periods, and is sensitive to shear stress and intracellular Mucin stores. *PLoS ONE*. 2015;10(5):e0127267.
81. Singhera GK, MacRedmond R, Dorscheid DR. Interleukin-9 and -13 inhibit spontaneous and corticosteroid induced apoptosis of normal airway epithelial cells. *Exp Lung Res*. 2008;34(9):579–598.
82. Tyner JW, et al. Blocking airway mucous cell metaplasia by inhibiting EGFR antiapoptosis and IL-13 transdifferentiation signals. *J Clin Invest*. 2006;116(2):309–321.
83. Aoshiba K, Rennard SI, Spurzem JR. Cell-matrix and cell-cell interactions modulate apoptosis of bronchial epithelial cells. *Am J Physiol*. 1997;272(1 Pt 1):L28–L37.
84. Gu Y, Rosenblatt J. New emerging roles for epithelial cell extrusion. *Curr Opin Cell Biol*. 2012;24(6):865–870.
85. Vermeer PD, Panko L, Karp P, Lee JH, Zabner J. Differentiation of human airway epithelia is dependent on erbB2. *Am J Physiol Lung Cell Mol Physiol*. 2006;291(2):L175–L180.
86. Vermeer PD, et al. MMP9 modulates tight junction integrity and cell viability in human airway epithelia. *Am J Physiol Lung Cell Mol Physiol*. 2009;296(5):L751–L762.
87. Adler KB, Tuvim MJ, Dickey BF. Regulated mucin secretion from airway epithelial cells. *Front Endocrinol (Lausanne)*. 2013;4:129.
88. Kim K, et al. Munc18b is an essential gene in mice whose expression is limiting for secretion by airway epithelial and mast cells. *Biochem J*. 2012;446(3):383–394.
89. Gutierrez BA, et al. Munc18-2, but not Munc18-1 or Munc18-3, controls compound and single-vesicle-regulated exocytosis in mast cells. *J Biol Chem*. 2018;293(19):7148–7159.
90. Jaramillo AM, et al. Different Munc18 proteins mediate baseline and stimulated airway mucin secretion. BioRxiv. https://doi.org/10.1101/451914. Published October 24, 2018. Accessed December 4, 2018.
91. Kamal A, Boehm MF, Burrows FJ. Therapeutic and diagnostic implications of Hsp90 activation. *Trends Mol Med*. 2004;10(6):283–290.
92. Schoof N, von Bonin F, Trümper L, Kube D. HSP90 is essential for Jak-STAT signaling in classical Hodgkin lymphoma cells. *Cell Commun Signal*. 2009;7:17.
93. Padmini E, Usha Rani M. Heat-shock protein 90 alpha (HSP90α) modulates signaling pathways towards tolerance of oxidative stress and enhanced survival of hepatocytes of Mugil cephalus. *Cell Stress Chaperones*. 2011;16(4):411–425.
94. Fukushima T, et al. HSP90 interacting with IRS-2 is involved in cAMP-dependent potentiation of IGF-I signals in FRTL-5 cells. *Mol Cell Endocrinol*. 2011;344(1-2):81–89.
95. Wang H, et al. Hsp90α forms a stable complex at the cilium neck for the interaction of signalling molecules in IGF-1 receptor signalling. *J Cell Sci*. 2015;128(1):100–108.
96. Deskin B, Lasky J, Zhuang Y, Shan B. Requirement of HDAC6 for activation of Notch1 by TGF-β1. *Sci Rep*. 2016;6:31086.
97. Chen G, et al. SPDEF is required for mouse pulmonary goblet cell differentiation and regulates a network of genes associated with mucus production. *J Clin Invest*. 2009;119(10):2914–2924.
98. Rajavelu P, Chen G, Xu Y, Kitzmiller JA, Korfhagen TR, Whitsett JA. Airway epithelial SPDEF integrates goblet cell differentiation and pulmonary Th2 inflammation. *J Clin Invest*.

2015;125(5):2021–2031.
99. Izuhara K, et al. Roles of periostin in respiratory disorders. *Am J Respir Crit Care Med*. 2016;193(9):949–956.
100. Krämer A, Green J, Pollard J, Tugendreich S. Causal analysis approaches in Ingenuity Pathway Analysis. *Bioinformatics*. 2014;30(4):523–530.
101. Acciani TH, Suzuki T, Trapnell BC, Le Cras TD. Epidermal growth factor receptor signalling regulates granulocyte-macrophage colony-stimulating factor production by airway epithelial cells and established allergic airway disease. *Clin Exp Allergy*. 2016;46(2):317–328.
102. Fossum SL, et al. Ets homologous factor (EHF) has critical roles in epithelial dysfunction in airway disease. *J Biol Chem*. 2017;292(26):10938–10949.
103. Nguyen HN, et al. Autocrine loop involving IL-6 family member LIF, LIF receptor, and STAT4 drives sustained fibroblast production of inflammatory mediators. *Immunity*. 2017;46(2):220–232.
104. Veldhoen M, Stockinger B. TGFbeta1, a "Jack of all trades": the link with pro-inflammatory IL-17-producing T cells. *Trends Immunol*. 2006;27(8):358–361.
105. Veldhoen M, Hocking RJ, Atkins CJ, Locksley RM, Stockinger B. TGFbeta in the context of an inflammatory cytokine milieu supports de novo differentiation of IL-17-producing T cells. *Immunity*. 2006;24(2):179–189.
106. Li JK, et al. IL-17 mediates inflammatory reactions via p38/c-Fos and JNK/c-Jun activation in an AP-1-dependent manner in human nucleus pulposus cells. *J Transl Med*. 2016;14:77.
107. Gupta A, Hossain MM, Miller N, Kerin M, Callagy G, Gupta S. NCOA3 coactivator is a transcriptional target of XBP1 and regulates PERK-eIF2α-ATF4 signalling in breast cancer. *Oncogene*. 2016;35(45):5860–5871.
108. Yu C, York B, Wang S, Feng Q, Xu J, O'Malley BW. An essential function of the SRC-3 coactivator in suppression of cytokine mRNA translation and inflammatory response. *Mol Cell*. 2007;25(5):765–778.
109. Amatya N, Garg AV, Gaffen SL. IL-17 Signaling: the yin and the yang. *Trends Immunol*. 2017;38(5):310–322.
110. Kalinowski A, et al. EGFR activation suppresses respiratory virus-induced IRF1-dependent CXCL10 production. *Am J Physiol Lung Cell Mol Physiol*. 2014;307(2):L186–L196.
111. Ueki IF, et al. Respiratory virus-induced EGFR activation suppresses IRF1-dependent interferon λ and antiviral defense in airway epithelium. *J Exp Med*. 2013;210(10):1929–1936.
112. Koff JL, Shao MX, Ueki IF, Nadel JA. Multiple TLRs activate EGFR via a signaling cascade to produce innate immune responses in airway epithelium. *Am J Physiol Lung Cell Mol Physiol*. 2008;294(6):L1068–L1075.
113. Ray A, Kolls JK. Neutrophilic inflammation in asthma and association with disease severity. *Trends Immunol*. 2017;38(12):942–954.
114. Reid AT, et al. Persistent induction of goblet cell differentiation in the airways: therapeutic approaches. *Pharmacol Ther*. 2018;185:155–169.
115. Berry MA, et al. Evidence of a role of tumor necrosis factor alpha in refractory asthma. *N Engl J Med*. 2006;354(7):697–708.
116. Erin EM, et al. The effects of a monoclonal antibody directed against tumor necrosis factor-alpha in asthma. *Am J Respir Crit Care Med*. 2006;174(7):753–762.
117. Holgate ST, et al. Efficacy and safety of etanercept in moderate-to-severe asthma: a randomised, controlled trial. *Eur Respir J*. 2011;37(6):1352–1359.
118. Wenzel SE, et al. A randomized, double-blind, placebo-controlled study of tumor necrosis factor-alpha blockade in severe persistent asthma. *Am J Respir Crit Care Med*. 2009;179(7):549–558.
119. Lai BT, Chin NW, Stanek AE, Keh W, Lanks KW. Quantitation and intracellular localization of the 85K heat shock protein by using monoclonal and polyclonal antibodies. *Mol Cell Biol*. 1984;4(12):2802–2810.
120. Schopf FH, Biebl MM, Buchner J. The HSP90 chaperone machinery. *Nat Rev Mol Cell Biol*. 2017;18(6):345–360.
121. Sanchez ER. Chaperoning steroidal physiology: lessons from mouse genetic models of Hsp90 and its cochaperones. *Biochim Biophys Acta*. 2012;1823(3):722–729.
122. Sreedhar AS, Kalmár E, Csermely P, Shen YF. Hsp90 isoforms: functions, expression and clinical importance. *FEBS Lett*. 2004;562(1-3):11–15.
123. Grad I, et al. The molecular chaperone Hsp90α is required for meiotic progression of spermatocytes beyond pachytene in the mouse. *PLoS ONE*. 2010;5(12):e15770.
124. Voss AK, Thomas T, Gruss P. Mice lacking HSP90beta fail to develop a placental labyrinth. *Development*. 2000;127(1):1–11.
125. Prince TL, et al. Client proteins and small molecule inhibitors display distinct binding preferences for constitutive and stress-induced HSP90 isoforms and their conformationally restricted mutants. *PLoS ONE*. 2015;10(10):e0141786.
126. Burgess DJ. Gene expression: More roles and details for polymerase pausing. *Nat Rev Genet*. 2012;13(7):450–451.
127. Siegal ML, Rushlow C. Pausing on the path to robustness. *Dev Cell*. 2012;22(5):905–906.
128. Sawarkar R, Sievers C, Paro R. Hsp90 globally targets paused RNA polymerase to regulate gene expression in response to environmental stimuli. *Cell*. 2012;149(4):807–818.
129. Calderwood SK, Neckers L. Hsp90 in cancer: transcriptional roles in the nucleus. *Adv Cancer Res*. 2016;129:89–106.
130. Panaretou B, et al. ATP binding and hydrolysis are essential to the function of the Hsp90 molecular chaperone in vivo. *EMBO J*. 1998;17(16):4829–4836.
131. Barzilay E, et al. Geldanamycin-associated inhibition of intracellular trafficking is attributed to a co-purified activity. *J Biol Chem*. 2004;279(8):6847–6852.
132. Kamal A, et al. A high-affinity conformation of Hsp90 confers tumour selectivity on Hsp90 inhibitors. *Nature*. 2003;425(6956):407–410.
133. Engelhardt JF, Schlossberg H, Yankaskas JR, Dudus L. Progenitor cells of the adult human airway involved in submucosal gland development. *Development*. 1995;121(7):2031–2046.
134. Turner J, et al. Goblet cells are derived from a FOXJ1-expressing progenitor in a human airway epithelium. *Am J Respir Cell Mol Biol*. 2011;44(3):276–284.
135. Boucherat O, Chakir J, Jeannotte L. The loss of Hoxa5 function promotes Notch-dependent goblet cell metaplasia in lung airways. *Biol Open*. 2012;1(7):677–691.
136. Evans CM, et al. Mucin is produced by clara cells in the proximal airways of antigen-challenged mice. *Am J Respir Cell Mol Biol*. 2004;31(4):382–394.
137. Hayashi T, Ishii A, Nakai S, Hasegawa K. Ultrastructure of goblet-cell metaplasia from Clara cell in the allergic asthmatic airway inflammation in a mouse model of asthma in vivo. *Virchows Arch*. 2004;444(1):66–73.
138. Reader JR, et al. Pathogenesis of mucous cell metaplasia in a murine asthma model. *Am J Pathol*. 2003;162(6):2069–2078.
139. Lafkas D, et al. Therapeutic antibodies reveal Notch control of transdifferentiation in the adult lung. *Nature*. 2015;528(7580):127–131.
140. Sidera K, Patsavoudi E. HSP90 inhibitors: current development and potential in cancer therapy. *Recent Pat Anticancer Drug Discov*. 2014;9(1):1–20.
141. Ma J, Rubin BK, Voynow JA. Mucins, Mucus, and Goblet Cells. *Chest*. 2018;154(1):169–176.
142. Karp PH, et al. An in vitro model of differentiated human airway epithelia. Methods for establishing primary cultures. *Methods Mol Biol*. 2002;188:115–137.
143. Schindelin J, et al. Fiji: an open-source platform for biological-image analysis. *Nat Methods*. 2012;9(7):676–682.
144. Schneider CA, Rasband WS, Eliceiri KW. NIH Image to ImageJ: 25 years of image analysis. *Nat Methods*. 2012;9(7):671–675.
145. Mishra A, Hogan SP, Brandt EB, Rothenberg ME. An etiological role for aeroallergens and eosinophils in experimental esophagitis. *J Clin Invest*. 2001;107(1):83–90.
146. Hallgren KA. Computing Inter-Rater Reliability for Observational Data: An Overview and Tutorial. *Tutor Quant Methods Psychol*. 2012;8(1):23–34.
147. Huber W, et al. Orchestrating high-throughput genomic analysis with Bioconductor. *Nat Methods*. 2015;12(2):115–121.
148. R Core Team. R: A language and environment for statistical computing, Vienna, Austria. https://www.R-project.org/. Accessed December 4, 2018.
149. Gamer M, Lemon J, Fellows I, Singh P. irr: Various Coefficients of Interrater Reliability and Agreement. R Project. https://CRAN.R-project.org/package=irr. Published July 16, 2012. Accessed December 4, 2018.
150. Light RJ. Measures of response agreement for qualitative data — some generalizations and alternatives. *Psychol Bull*. 1971;76(5):365–377.
151. Edgar R, Domrachev M, Lash AE. Gene Expression Omnibus: NCBI gene expression and hybridization array data repository. *Nucleic Acids Res*. 2002;30(1):207–210.
152. Barrett T, et al. NCBI GEO: archive for functional genomics data sets--update. *Nucleic Acids Res*. 2013;41(Database issue):D991–D995.
153. Bray NL, Pimentel H, Melsted P, Pachter L. Near-optimal probabilistic RNA-seq quantification. *Nat Biotechnol*. 2016;34(5):525–527.
154. Pimentel H, Bray NL, Puente S, Melsted P,

Pachter L. Differential analysis of RNA-seq incorporating quantification uncertainty. *Nat Methods*. 2017;14(7):687–690.
155. Soneson C, Love MI, Robinson MD. Differential analyses for RNA-seq: transcript-level estimates improve gene-level inferences. *F1000Res*. 2015;4:1521.
156. Love MI, Huber W, Anders S. Moderated estimation of fold change and dispersion for RNA-seq data with DESeq2. *Genome Biol*. 2014;15(12):550.
157. Gu X, et al. Reduced PDEF expression increases invasion and expression of mesenchymal genes in prostate cancer cells. *Cancer Res*. 2007;67(9):4219–4226.
158. Tilman G, Mattiussi M, Brasseur F, van Baren N, Decottignies A. Human periostin gene expression in normal tissues, tumors and melanoma: evidences for periostin production by both stromal and melanoma cells. *Mol Cancer*. 2007;6:80.
159. Vandesompele J, et al. Accurate normalization of real-time quantitative RT-PCR data by geometric averaging of multiple internal control genes. *Genome Biol*. 2002;3(7):RESEARCH0034.
160. Metsalu T, Vilo J. ClustVis: a web tool for visualizing clustering of multivariate data using principal component analysis and heatmap. *Nucleic Acids Res*. 2015;43(W1):W566–W570.